# GLOBAL MAPPING OF UNDERWATER UV IRRADIANCES AND DNA-WEIGHTED EXPOSURES USING TOMS AND SEAWIFS DATA PRODUCTS

Alexander Vasilkov[1], Nickolay Krotkov[1], Jay Herman[2], Charles McClain[2], Kevin Arrigo[3], and Wayne Robinson[4]

**Abstract.** The global stratospheric ozone-layer depletion results in an increase in biologically harmful ultraviolet (UV) radiation reaching the surface and penetrating to ecologically significant depths in natural waters. Such an increase can be estimated on a global scale by combining satellite estimates of UV irradiance at the ocean surface from the Total Ozone Mapping Spectrometer (TOMS) satellite instrument with the SeaWiFS satellite ocean-color measurements in the visible spectral region. In this paper we propose a model of seawater optical properties in the UV spectral region based on the Case 1 water model in the visible range. The inputs to the model are standard monthly SeaWiFS products: chlorophyll concentration and the diffuse attenuation coefficient at 490nm. Penetration of solar UV radiation to different depths in open ocean waters is calculated using the RT (radiative transfer) quasi-single scattering approximation (QSSA). The accuracy of the QSSA approximation in the water is tested using more accurate codes. The sensitivity study of the underwater UV irradiance to atmospheric and oceanic optical properties have shown that the main environmental parameters controlling the absolute levels of the UVB (280-320nm) and DNA-weighted irradiance underwater are: solar-zenith angle, cloud transmittance, water optical properties, and total ozone. Weekly maps of underwater UV irradiance and DNA-weighted exposure are calculated using monthly-mean SeaWiFS chlorophyll and diffuse attenuation coefficient products, daily SeaWiFS cloud fraction data, and the TOMS-derived surface UV irradiance daily maps. The final products include global maps of weekly-average UVB irradiance and DNA-weighted daily exposures at 3m and 10m, and depths where the UVB irradiance and DNA-weighted dose rate at local noon are equal to 10% of their surface values.

## 1. Introduction

Increased levels of biologically harmful UV-B radiation (280-320nm) resulting from the depletion of Earth's ozone layer [*WMO*, 1999; *Herman et al.*, 1996] have been shown to affect aquatic ecosystems. One of the important effects of enhanced levels of UVB radiation is a reduction in the productivity of phytoplankton caused by their moving to increased depths where there is less PAR (photosynthetic active radiation). This effect has been conclusively confirmed in the laboratory [*Worrest and Hader*, 1989] and from field observations in the Bellinghausen Sea (Antarctica). *Smith et al.* [1992] compared the productivity of Antarctic phytoplankton beneath and outside the Antarctic ozone hole and reported a 6-12% loss due to enhanced UVB. Other studies report smaller effects,

[1] Raytheon ITSS, Lanham, Maryland.
[2] NASA Goddard Space Flight Center, Greenbelt, Maryland.
[3] Department of Geophysics, Stanford University, Stanford, California
[4] SAIC General Sciences Co. and NASA/GSFC SeaWiFS Project, Greenbelt, Maryland.

generally ranging from 1% [*Arrigo*, 1994] to 5% [*Neale et al.* 1998a, b; *Holm-Hansen et al.* 1993]. Enhanced UVB radiation could also affect the photochemical production of carbonyl sulfide (COS) in seawater [*Zepp and Andreae*, 1994], thereby augmenting the greenhouse effect and affecting other long-term global biogeochemical cycles.

The quantitative assessment of UV effects on aquatic organisms on a global scale requires an estimate of the in-water radiation field. The total ozone and UV reflectivity measurements from the Total Ozone Mapping Spectrometer (TOMS) satellite instruments allow calculation of global daily UV irradiance at the ocean surface [*Eck et al.* 1995; *Herman et al.* 1996; *Krotkov* et al. 1998; *Herman et al.* 1999]. Because of long time record (since 1978) and contiguous global spatial coverage, TOMS data are vital not only for estimating zonal average trends in surface UV irradiance [*Madronich 1992; Herman et al. 1996*], but also in studying geographical differences in surface UV climatology [*Herman et al., 1999; WMO 1999*]. The current TOMS instrument onboard NASA's Earth-Probe satellite has been collecting data since July 1996, and is expected to continue ozone and surface UV reflectivity measurements to provide overlap with launch of the last TOMS instrument (July 2000). Additional spaceborne ozone sensors are planned by the United States and other countries well through the next century (Global Ozone Monitoring Experiment (GOME) on European ERS-2 satellite, Triana-EPIC (Earth Polychromatic Imaging Camera), and Ozone Monitoring Instrument (OMI) on NASA's EOS-CHEM satellite).

Estimates of UV transmission in ocean surface waters require knowledge of the inherent and apparent optical properties of seawater. For ocean properties, the Coastal Zone Color Scanner flown onboard NASA's Nimbus-7 satellite and current ocean-color satellite instruments, such as NASA's SeaWiFS instrument (Sea-viewing Wide Field-of-view Sensor, Hooker et al., 1992) were designed to provide frequent global measurement of the water-leaving radiances from which inherent water optical properties (IOP) and constituents (Chlorophyll concentration) can be inferred.

The main goal of this paper is to estimate the penetration of UV light into Case I open ocean waters using large-scale TOMS surface-UV and SeaWiFS ocean-color measurements. In assimilating these satellite data sets, two major problems arise: the fast radiative transfer modeling of the penetration of UV light into the water and extrapolation of water optical properties derived from the satellite visible channels to the UV spectral region. The paper discusses both problems with focus on the "radiative transfer" (RT) part. In section 2 we briefly discuss the SeaWiFS and TOMS data as input to the RT models. Section 3 discusses the water RT model in more details as well as the parameterization of the UV optical properties for Case I water. The accuracy of the water RT approximation is tested using well-established accurate models (*Mobley et al.*, 1993). Section 4 discusses the calculated maps of underwater UV irradiance including the depth dependence of the UV dose rates for UVB and unshielded DNA. The sensitivity study to water optical properties is also discussed.

## 2. Satellite Data

The general algorithm (data flow) for incorporating both TOMS and SeaWiFS satellite data into radiative transfer models is shown in Figure 1. In section 2.1 we discuss the SeaWiFS data in more detail. Section 2.2 discusses TOMS surface-UV product.

### 2.1 SeaWiFS data

We use the Level 3 binned monthly mean SeaWifs data for estimates of chlorophyll concentration and the diffuse attenuation coefficient $K_d$(490nm), as well as the daily SeaWiFS cloud fraction data. The SeaWiFS instrument has 8 bands between 412 nm and 865 nm [*Barnes, et al.*, 1994], and is in descending (North to South) noontime sun-synchronous orbit. The orbit and swath characteristics allow global coverage every two days, with gaps between consecutive swaths at low latitudes being filled the following day. The inherent resolution of the instrument is about 1 km at nadir, but the coverage is subsampled on-board the spacecraft to provide 4 km global area coverage (GAC). The global coverage includes both land and ocean areas, but is limited to solar zenith angles less than $70^0$ to conserve spacecraft power. The GAC data is processed at the SeaWiFS Project Office in near-realtime.

The stability of the sensor is tracked using a time series of monthly lunar calibration images [*Barnes, et al.*, 1999]. The prelaunch laboratory calibrations [*Johnson, et al.*, 1999] are adjusted so that the derived water-leaving radiances in bands 1-6 (412 nm - 670 nm) are matched to field measurements collected by the Marine Optical Buoy (MOBY) located off Lanai, Hawaii [*McClain, et al.*, 1998]. The calibrated radiances (Level-1) over the ocean are atmospherically corrected [*Gordon and Wang*, 1994] to derive Level-2 geophysical products, e.g., normalized water-leaving radiances [*Gordon and Clark*, 1982], chlorophyll-*a* [*O'Reilly, et al.*, 1997], and diffuse attenuation coefficient at 490 nm, $K_d$(490), [*Mueller and Trees*, 1997]. These data are spatially binned and averaged on a 9 km global grid (Level-3) for each day. The daily gridded data is temporally averaged at 8-day, monthly, and annual periods. Figures 2 and 3 show the July 1998 monthly-average chlorophyll and $K_d$(490) fields. *McClain, et al.* [1998] presented the initial validation of the chlorophyll retrievals in Case 1 waters, i.e., waters where the reflectance is determined by absorption. Further analyses using a larger data set supports the initial evaluations that the chlorophyll retrievals are within the SeaWiFS accuracy goal (± 35% for Case 1 waters) [*Hooker and McClain*, 1999].

For underwater irradiance calculations, one needs to know both the direct and diffuse components of the surface irradiance, and the boundary conditions at the air-water interface. For ocean water, the boundary conditions are largely determined by wind speed. The TOMS standard data (described below) provides only the global surface irradiance (diffuse plus direct). To calculate the daily-average direct irradiance, information on average cloud fraction in each grid-cell is required. Such information is obtained from the 865nm channel of the SeaWiFS sensor.

The SeaWiFS cloud-albedo threshold over ocean was set at 1.1% [*Arrigo and McClain* 1995]. The relation is a binary one: if the threshold is crossed, the SeaWiFS GAC pixel (4km by 4km) is declared cloud contaminated and the cloud flag is set for that pixel.

During binning, if the flag is set, that sample is considered to be 100% cloud, otherwise 0%. The threshold albedo of 1.1% agrees with model calculations of reflected radiance for spectral band 0.82-0.88μm above the ocean for a clear atmosphere (the normalized reflection coefficient (albedo) is in the range 0.5-1% for clear Rayleigh atmosphere and 2- 4% including haze and thin cirrus clouds effects). The current cloud flag also masks sun glint, high aerosols, and thin cirrus clouds.

Figure 4 shows a 5-day average SeaWiFS cloud fraction map averaged over 1 by 1 deg grid cells. Because of the conservative cloud flag threshold required by the SeaWiFS ocean color algorithm, there are relatively small amounts of clear regions (Mediterranian, Tropical Atlantic Region, and Equatorial Pacific belt). On the other hand, regions declared to have 100% cloud cover may actually contain aerosol plumes that originated on land (Sahara Region) and were transported over open ocean regions [Herman et al., 1997].

## 2.2 TOMS data

TOMS measures solar radiation backscattered from the Erath's atmosphere in 6 narrow (~1nm) wavelength channels (308, 312, 317, 322, 331, and 360nm for Earth-Probe, July 1996 to present, and 312, 317, 331, 340, 360, and 380 nm for Nimbus-7, November 1978 to April 1993). This information is converted into total column ozone amounts, scene reflectivity, aerosol amounts, and cloud transmittance [*McPeters et al.*, 1996]. The Level 2 TOMS products are obtained for areas corresponding to the satellite field of view (FOV) on the Earth's surface (~40 km by 40km in nadir direction for EP/TOMS since January 1998 to the present). Since the TOMS orbit is Sun synchronous, the FOV can be combined into a global map of the same parameters at the same solar time every day (Level 3 products). Because of the accurate in-flight calibrations and long-term stability of the instrument, the TOMS satellite products are able to maintain absolute and relative accuracy over wide-geographical areas and long periods.

The TOMS daily gridded (Level 3) products (ozone, reflectivity and aerosol index) are used as an input for a radiative transfer model to generate daily global maps of the surface global (direct plus diffuse) spectral irradiance at the satellite overpass time [*Krotkov et al.*, 1998; *Herman et al.*, 1999]. To calculate daily UV exposures we use cloud and aerosol amounts at the overpass time, but neglect their diurnal variation. Detailed information about TOMS products and daily erythemal maps of the surface UV can be found on the TOMS web site: http://toms.gsfc.nasa.gov and in the TOMS User's Guide [*McPeters et al., 1998*].

The accuracy of estimated UV exposure (time integrated UV irradiance) at a specific location is limited by the coarse spatial resolution of the TOMS observations and the satellite's ability to obtain only one UV irradiance estimate per day (except for high latitudes). Because of the highly variable nature (temporal and spatial) of cloud and aerosol cover the TOMS daily UV estimations should be averaged over periods of at least a week to obtain a good estimate of the accumulated UV exposure [*Herman et al.*, 1999].

For the purposes of estimating UV irradiance at the Earth's surface, there are two classes of aerosols that must be considered: 1) aerosols that only scatter UV radiation and 2) aerosols that both scatter and absorb UV radiation. The first category is included in the TOMS measured scene reflectivity, and attenuates UV radiation in a manner that very closely approximates clouds of equivalent reflectivity. Attenuation values of up to 10% are common.

The second category, absorbing aerosols, must be treated separately. First, clouds are distinguished from aerosols by use of the TOMS aerosol index (AI) technique [*Herman et al.*, 1997 *Torres et al.*, 1998]. Specifically, the AI is zero for water clouds, positive for absorbing aerosols, and negative for non-absorbing aerosols (e.g., sulfate aerosols). The AI is available from standard TOMS data, as a byproduct of the total ozone retrieval algorithm. The AI data can be used directly to correct surface irradiance for attenuation by absorbing aerosol plumes, if the aerosol altitude is known from either direct measurement or climatological estimates:

$$\frac{F_{aerosol}}{F_{Clear}} = e^{-g(H_A)AI} \qquad (1)$$

where the conversion factor g is a function of aerosol height, $H_A$ [*Krotkov et al.*, 1998; *Herman et al*, 1999]. One method for obtaining $H_A$ is by using the GSFC wind-data assimilation model to estimate aerosol plume heights by matching modeled and observed plume trajectories over several days. This method, and comparisons with sunphotometer data, show that the aerosol plumes are usually located between 3 and 4 km altitude, and are repetitive at a given location from year to year. Error estimates for uncertainties in $H_A$ are given in *Herman et al.* [1999].

## 3. Model

The atmospheric RT model provides the boundary conditions at the ocean surface for the underwater irradiance calculation. The radiative transfer solutions in the atmosphere and in the ocean are coupled through the contribution of photons first reflected from the ocean and then scattered back to the water by the atmosphere. The ocean contribution to the downward clear-sky irradiance, $F_{clear}(\lambda)$, can be estimated from the following equation:

$$F_{clear}(\lambda) = F_0(\lambda)\,(1+\Gamma)/(1-A\,S_b(\lambda)) \qquad (2)$$

where $A$ is the ocean albedo, $F_0$ is direct irradiance at the surface for $A$=0, $\Gamma$ is the ratio of diffuse to direct irradiance at the surface for $A$=0 and $S_b(\lambda)$ is the fraction of reflected radiation backscattered to the ocean by the atmosphere [Herman et al., 1999]. $\Gamma$ and $S_b(\lambda)$ were calculated for a clear atmosphere that contains Rayleigh scatterers and ozone using DISORT code [*Stamnes et al.*, 1988]. Given the maximum value of $S_b$=0.4 for a clear sky and ocean albedo values less than 10% in the near UV region [*Herman and Celarier*, 1997], one can neglect the coupling of the atmospheric and oceanic radiative transfer as a

first approximation. We estimate that the flat ocean surface model and the separation of the atmospheric and oceanic RT models both give less than 10% resulting error for satellite estimation of the underwater UV irradiance.

### 3.1 Surface UV calculation

The combined TOMS datasets, along with the satellite measured high-resolution extraterrestrial solar irradiance spectra, are used as an input to our atmospheric radiative transfer model to calculate surface UV irradiance at the time of the satellite overpass (approximately 1100 LT for Earth-Probe / TOMS). Using daily measurements of ozone from TOMS, equation (2) is applied to calculate $F_{clear}$ at the surface for clear-sky and aerosol-free conditions. The direct radiation is calculated from Beer's law with airmass correction for high solar zenith angle ($\theta < 75^{o}$). The parameters $\Gamma$ and $S_b$ are interpolated from a look-up table pre-calculated for a Rayleigh atmosphere using climatological TOMS 325DU ozone and temperature profiles for different solar zenith angles, assuming an average ocean albedo of 6% at 360nm. The angular distribution of the downward radiance at the air-ocean boundary is assumed isotropic with a flat ocean surface (Fresnel refraction). The absolute irradiances were obtained using extraterrestrial solar irradiance data, acquired by the SOLSTICE [*Rottman et al.*, 1993] instrument on NASA's Upper Atmospheric research Satellite (UARS).

A simple model to account for reduction of $F_{clear}$ caused by clouds over a low reflecting ocean surface is based on an energy balance between solar radiation reaching the ground and backscatered to space. For this model [*Eck et al.*, 1995; *Herman et al.*, 1996; *Herman et al.*, 1999]:

$$F_{cloud} = F_{clear}\, C_T$$

$$C_T \sim 1 - (R_{360} - 0.06)/0.88 \quad \text{for } 0.06 < R_{360} < 0.5 \qquad (3)$$

$$C_T = 1 - R_{360} \quad \text{for } R_{360} > 0.5$$

This equation accounts for UV irradiance reduction from both clouds and non-absorbing aerosols, but needs an additional correction in the presence of absorbing aerosol plumes, where UV irradiance reduction is stronger. When plumes of absorbing aerosols are detected in the TOMS AI data, the UV irradiance is corrected using Equation (1) [*Krotkov et al.*, 1998]. Typical levels of UV reduction can be up to 50% under Saharan dust and the annual smoke plumes from Africa and South America. This reduction can reach 90% for dense smoke near the fire source and for unusual conditions such as occurred in Indonesia and Mexico during 1998 and early 1999 [*Herman et al.*, 1999].

The daily UV dose is calculated by integrating over time and assuming that $C_T$ is constant throughout the day. This daily cloud variability error is assumed random, therefore it is reduced with weekly averaging of daily exposures. Figure 5 shows the 10-day average TOMS daily erythemal [*McKinlay and Fiffey*, 1987] exposure map including the combined effects of ozone, clouds and absorbing aerosols [*Herman et al.*, 1999]. The

most pronounced effect is the dependence on solar zenith angle, θ so that geographical areas whose latitudes are near sub-solar points (e.g., +23N for July) produce very high clear-sky surface UV irradiance. The next strongest source of surface UV modulation is from clouds. In July, there is considerable haze and clouds over the ocean areas in the Northern Hemisphere, since the Intertropical Convergence Zone (ITCZ) cloud region has moved toward the north. Interhemispheric differences in cloud cover cause the Southern Hemisphere summer to have even higher exposures than the Northern Hemisphere summer for the same SZA [*Herman et al.*, 1999]. The remaining geographical variations can be attributed to ozone variations and absorbing aerosols in certain regions.

To provide boundary condition to the underwater RT, we must separate the TOMS estimated global irradiance ($F_{cloud}$) into direct and diffuse components. The direct component is estimated using the SeaWiFS cloud fraction data, $S_{CF}$ (in percent):

$$F_{direct} = F_0(\lambda)\,(1 - 0.01\,S_{CF}) \tag{4}$$

Finally, the diffuse component at the surface is determined as the residue between the TOMS global irradiance, $F_{Cloud}$, and the direct component estimated from SeaWiFS cloud fraction in equation 3:

$$F_{diffuse} = F_{cloud} - F_{direct} \tag{5}$$

### 3.2. Radiative transfer in the ocean

Given the TOMS estimate of the surface UV irradiance, and assuming isotropic angular distribution of the diffuse downward radiance at the ocean surface, any appropriate radiative transfer scheme can be applied to model light penetration into the ocean [*Jin and Stamnes*,1994; *Mobley et al.*, 1993]. However, the accuracy of the current optical measurements of the most fundamental inherent optical properties of seawater (scattering and absorption coefficients) is normally about 10%, and the errors of extrapolation of these properties into UV spectral region has yet to be estimated. This currently prevents us from applying these sophisticated radiative transfer schemes for the purpose of operational satellite mapping of underwater UV fields. However, the accurate models [*Mobley et al.*, 1993] are very important for testing faster operational algorithms.

#### 3.2.1. The Quasi-single scattering approximation of radiation transfer in water

The first model for an assessment of underwater UV radiation and biodoses was developed by *Smith and Baker* [1979]. In this model it was assumed that the irradiance is attenuated exponentially in the ocean: $E_\lambda(z) = E_\lambda^0 \exp(-K_d z)$, where $E_\lambda^0$ and $E_\lambda(z)$ are spectral irradiances just below the ocean surface and at depth, $z$ (we use different notation $E$ for irradiances within the ocean to distinguish them from the atmospheric irradiances: $F$), and the diffuse attenuation coefficient, $K_d$ , is assumed to be vertically constant. A similar model was applied by *Booth et al.* [1992]. This simple formulation of the

radiative transfer in the ocean requires an a-priori knowledge of $K_d$ in the UV spectral region.

In general, $K_d$ cannot be extrapolated from the visible region for use in the UV wavelengths. The coefficient $K_d$ depends on the angular structure of the light field and, thus, on depth (even for a homogeneous ocean), and on seawater inherent optical properties (IOPs). Therefore, there is no a-priori reason to expect that $K_d$ values in the UV region will vary in the same manner with the angular structure of the light field and depth as in the visible region. However, in some ocean areas this correlation was reported. For example, *Hojerslev and Aas* (1991) have shown that $K_d(310)$ is linearly correlated to $K_d(465)$ for vast ocean areas with the correlation coefficient as large as 0.998. The problem of correlation between spectral values of the diffuse attenuation coefficient is carefully discussed by Hojerslev [1982, 1986]. From the theoretical point of view the relationship between the diffuse attenuation coefficient and seawater IOPs is considered by Gordon [1989].

To calculate UV underwater irradiances, we chose here the, so-called, Quasi-Single Scattering Approximation (QSSA) [*Gordon*, 1973]. The QSSA model is important, because of its simple analytical formulation, yet enabling us to address the dependence of $K_d$ on the angular distribution of the light field in the ocean. Thus, the model can account for $K_d$ dependence on depth even in vertically homogeneous water. The QSSA is based on the strong absorption with highly anisotropic scattering of seawater [*Gordon*, 1973]. It assumes: (a) single scattering in the upward direction; (b) multiple scattering in the downward direction in accordance with delta-function. The approximation assumes the exponential direct-beam transmittance: $T_b = exp(-Kz/\mu)$, where $K = a + b'_b$ is the effective attenuation coefficient, $a$ is the absorption coefficient, $b'_b$ is the fraction of backscatter in the upward direction, and $\mu$ is the cosine of the zenith angle of incident beam. The fraction of backscatter in the upward direction is exactly equal to the backscattering coefficient, $b_b$, in the case of normal incident beam, i.e. $\mu=1$. In-water zenith angles are limited by the angle of total internal reflection. Accounting for this fact, and the small contribution of backscatter to total attenuation of light, we assume that $b'_b \equiv b_b$.

Here the water column is assumed to be vertically homogeneous. This assumption can be easily accepted because the penetration depth for UV radiation does not ordinary exceed the depth of the upper quasi-homogeneous, well-mixed layer in the ocean. The spectral irradiance at depth, z, can be written as a sum of the direct solar radiation and the integral of surface radiance over spherical angles from the diffuse radiation, both attenuated by water [*Krotkov and Vasilkov*, 1993]:

$$E_\lambda(z) = E_\lambda^0\, T_b(\mu_0) \; + \int_0^{2\pi} d\varphi \int_0^{\mu_1} L_\lambda(\mu,\varphi)\, T_b(\mu)\; \mu\, d\mu \qquad (6)$$

where $E_\lambda^0$ is the spectral irradiance for direct solar radiation just beneath the ocean surface, $\mu_0$ is the cosine of the solar zenith angle in the water, $\varphi$ is the azimuth angle, $\mu_1$ is

the cosine of the total internal reflection angle ~$49^0$, $L_\lambda(\mu,\varphi)$ is the angular distribution of sky radiance after surface refraction and reflection.

### 3.2.2. Model of seawater inherent optical properties (IOPs)

The QSSA makes use of the absorption coefficient, $a$, and the backscattering coefficient, $b_b$. The total IOPs are the sums of the IOP of the pure seawater and the three major scattering and absorbing water substances:

$$a(\lambda) = a_w(\lambda) + a_{DOM}(\lambda) + a_{Ph}(\lambda), \quad b_b(\lambda) = b_W(\lambda) + b_p(\lambda) \qquad (7)$$

where subscripts *w, p, ph* and *DOM* denote the pure seawater, the particulate matter, the phytoplankton pigments, and dissolved organic mater (DOM), respectively. The detritus absorption is included into the DOM absorption because of approximately identical spectral dependence [*Carder et al.*, 1991].

The pure seawater IOPs were obtained from *Smith and Baker* [1981]. According to the recent findings [*Pope and Fry*, 1997; *Sogandares and Fry*, 1997] the pure water absorption coefficient is significantly below the consensus values (as previously selected by *Smith and Baker* [1981] ) in the wavelength range 380 – 500 nm, about 2 times lower than the old value at 380nm. Currently, no revised measurements of the pure-water absorption coefficients are available for wavelengths shorter than 340nm. Therefore, for the present paper we use values of the pure-seawater absorption coefficient from *Smith and Baker* [1981] in most calculations.

The suspended particulate matter (SPM) backscattering coefficient and the DOM absorption coefficient are used in the conventional form:

$$a_{DOM}(\lambda) = a_0 \exp[-S(\lambda-\lambda_0)], \quad b_b(\lambda) = b_0(\lambda/\lambda_0)^{-m} \qquad (8)$$

where $m$ is the backscatter wavelength ratio exponent, $S$ is the DOM spectral slope.

The DOM spectral slope $S$=0.014 $nm^{-1}$ is commonly accepted for the visible spectral region [*Bricaud et al.*, 1981]. A study by *Kopelevich et al.* [1989] showed that the DOM spectral slope should be put slightly greater in the 280-490 nm spectral region: $S$=0.017 ±0.001 $nm^{-1}$. More recent measurements have showed that the DOM spectral slope can increase with photodegradation of colored DOM and can vary within a rather wide range from 0.01 to 0.03 $nm^{-1}$ for clear waters [*Vodacek and Blough*, 1997]. Unfortunately, these variations of the DOM spectral slope have not been parameterized. We use, therefore, an average value of the DOM spectral slope for the UV spectral region $S$=0.017 $nm^{-1}$. The parameter $m$ may vary in a wide range depending on the optical type of seawater. Fortunately, the SPM backscattering coefficient, $b_0$, is normally much less than the total absorption coefficient, $a$, in the UV spectral region. Therefore, an average estimate of the parameter $m$=1 was adopted in the model of *Gordon and Morel* [1983].

The phytoplankton pigment absorption is expressed through chlorophyll *a* concentration and the chlorophyll-specific absorption coefficient:

$$a_{Ph}(\lambda) = C\, a^*_{Ph}(\lambda) \qquad (9)$$

Phytoplankton synthesize a variety of compounds that absorb radiation in the UV-B and UV-A regions of the spectrum and which could affect the response of the cell to UV radiation. In vivo absorption in the UV-A and UV-B shows a wide range of values, with peaks of absorption between 320 and 350 nm and a maximum between 330 and 335 nm (Vernet et al., 1994). For all surface samples, the average in vivo pigment-specific UV absorption was larger than absorption in the blue. The overall variance was high, demonstrating that the absorption in the UV is not due to the major photosynthetic pigments and that the UV-absorbing compounds, such as mycosporine-like amino acids, vary independently. The average for all-stations spectrum was accepted to be the chlorophyll-specific absorption coefficient in the model. Values of the function $R(\lambda)=a_{ph}^*(\lambda) / a_{ph}^*(440)$ calculated on basis of this data are given in Table 1. Values of the function calculated in [*Kopelevich and Ershova*, 1997] are also given in Table 1 for comparison. As can be seen from Table 1 the values $A(\lambda)$ [*Kopelevich and Ershova*, 1997] are less than the values $R(\lambda)$ [*Vernet et al.*, 1994] even for the average minus standard deviation spectrum. We use the data of *Vernet et al.* [1994] in our calculations.

Table 1. The function $R(\lambda)$ calculated on basis of data of [*Vernet et al.*, 1994]

| *Wavelength, nm* | *380* | *360* | *340* | *331* |
|---|---|---|---|---|
| Average plus standard deviation spectrum | 0.81 | 0.90 | 1.56 | 1.80 |
| Average spectrum | 0.78 | 0.80 | 1.27 | 1.47 |
| Average minus standard deviation spectrum | 0.65 | 0.60 | 0.65 | 0.85 |
| after *Kopelevich and Ershova*, 1997 | 0.49 | 0.42 | 0.61 | 0.68 |

The model contains three input quantities: $a_0$, $b_0$, and $C$. These parameters are to be estimated from available satellite data sets. Some seawater characteristics can be retrieved in the visible spectral region using the data of satellite ocean color sensors. The problem of first importance is an extrapolation of the water absorption and scattering coefficients measured or retrieved from satellite measurements in the visible (400 – 600 nm) into the UV spectral region (290 – 400 nm). The above spectral model of IOPs allows such an extrapolation provided the model-input parameters are known and parameterization of IOPs is valid.

What should be definitely refined in the future is the parameterization of phytoplankton absorption. It is well known that the chlorophyll-specific absorption coefficient depends on chlorophyll concentration due to, for example, pigment packaging effect. This dependence has been parameterized for the visible range in *Bricaud et al.* [1995]. However, for the UV region, the more important issue may be a weak correlation between photosynthetic pigments and UV-absorbing, photoprotective pigments. Because of lack of such data, we chose a rather simple parameterization of the chlorophyll-specific absorption coefficient.

Next, we will consider how the model-input parameters can be estimated from available standard products of satellite ocean-color sensors. First, the chlorophyll concentration is the standard SeaWiFS product. To determine other quantities, the Case 1 water model [*Morel*, 1988] is assumed. According to the model, the DOM absorption at 440 nm is 20% of the total absorption of pure seawater and pigments. This assumption determines the most important parameter $a_0$. To estimate the backscattering coefficient we use the standard SeaWiFS product of the diffuse attenuation coefficient [*McClain et al.*, 1992] and the model of the diffuse attenuation coefficient developed in *Gordon* [1989]:

$$K_d / D_0 = 1.0395\,(a + b_b), \qquad (10)$$
$$D_0 = f / \cos\theta_{0w} + 1.197\,(1 - f),$$

where $f$ is the fraction of direct sunlight in the incident irradiance transmitted through the sea surface. The fraction $f$ is calculated as a function of solar zenith angle and wavelength from the atmospheric model.

Coastal waters are normally referred as Case 2 waters in which IOPs are uncorrelated. The above model cannot be directly applied to those waters. However, independent retrieval of absorption coefficients of DOM and phytoplankton pigments has been suggested in *Carder et al.*, [1991]; *Hoge and Lyon*, [1996]; *Garver and Siegel*, [1997] and *Vasilkov*, [1997]. Given the DOM absorption coefficient in the visible region, it can be extrapolated into the UV region. The SPM backscattering coefficient can also be retrieved using analytical algorithms [*Hoge and Lyon, 1996*; *Garver and Siegel*, 1997; *Vasilkov*, 1997].

### 3.2.3. Verification of the QSSA

The accuracy of the QSSA was estimated by comparison with the accurate RT calculations for the simplified models of the ocean. In this paper we used radiative transfer code intercomparisons [*Mobley et al.*,1993] and results of an accurate Monte-Carlo radiative transfer scheme [*Vasilkov et al.*, 1999]. The underwater irradiance was compared with data for Problem 2 from the paper by *Mobley et al.*, [1993]. The same scattering phase function was used in the QSSA calculation. The relative error of the QSSA within the optical depth range of 10 was less then 7% for the single scattering albedo $\omega$=0.2. For the single scattering albedo $\omega$=0.9, the QSSA error was 17% for the optical depth $\tau$=5 and 49% for the optical depth $\tau$=10.

Problem 2 [*Mobley et al.*, 1993] deals only with the direct solar radiation illuminating the surface. To estimate the errors of the QSSA in case of the diffuse illumination, Monte-Carlo calculations were conducted for an isotopic angular distribution of incident radiance on the ocean surface [*Vasilkov et al.*, 1999]. For a typical single scattering albedo $\omega$=0.6, the QSSA error was less than 35% in the optical depth region $\tau$<10. In all cases the errors were less at smaller optical depths. Similar results regarding the QSSA accuracy has been reported using Monte-Carlo simulations [*Greysukh and Levin*,1990].

It should be noted that certain conditions specific for UV spectral region justify the application of the QSSA to the radiative transfer problem in the water:

(a) $\omega$ is normally less than 0.7 in the UV spectral region and gets smaller at short wavelengths, which are more biologically effective;

(b) only small optical depths play a significant role in biological applications of the underwater UV calculations. All these considerations should permit the use of the QSSA for calculations of biologically significant parameters from the underwater UV irradiance.

## 4. Results

The biological effect of UV radiation is typically described by action spectra. A large number of action spectra, $A(\lambda)$, has been proposed for various biological effects of UV radiation in marine environment (for Antarctic waters see discussion by *Smith et al.* [1992]). Two action spectra with considerably different shapes have been chosen for a sensitivity study: (1) the marine phytoplankton [*Mitchell,* 1990] and (2) unshielded DNA (Setlow spectrum) [*Quaite et al.,* 1992]. We simulate the typically measured biological daily UV doses by convolution of UV irradiance spectra- $E_\lambda(z)$ with $A(\lambda)$ and integrating over the time of the day:

$$D(z) = \int dt \int_{280}^{400} E_\lambda(z, \mu_0(t))\, A(\lambda)\, d\lambda \qquad (11)$$

To estimate the damage for particular biological process, the units of $E_\lambda$ should agree with the units of $A(\lambda)$. For example, to model the conditions of the field experiments described in *Reagan et al.* [1992], we have chosen the action spectrum for unshielded DNA [*Quaite et al.,* 1992]. Since the $A(\lambda)$ is given in terms of number of pyrimidine dimers per photon/m$^2$, the value of $E_\lambda$ in W / (m$^2$nm) was transformed to quantum units as $E_{ph} = E_\lambda / hc$, where $h$ is the Plank constant and $c$ is the light speed. The calculations of $D(z=0)$ gave a value of 0.5% pyrimidine dimers for typical total column ozone values of 260DU near the Bahamas (23°45'N) in July 1990. This is close to the estimate by *Reagan et al.* [1992], that daily exposure of DNA molecules just above the surface produced 0.45% pyrimidine dimers (or 4.5 dimers per thousand bases of molecule). Unfortunately, no water optical properties were measured in the field experiment by *Reagan et al.* [1992], which prevents a comparison with underwater data.

### 4.1 DNA doses

The weekly averaged DNA dose at depth of 3 m is shown in Fig. 6. It is seen that the main features of the averaged DNA dose map are determined by latitude dependence of the surface UV irradiance. The latitude dependence of the DNA dose is clearly apparent in all oceans. Some features of the DNA dose map are due to cloudiness structure. For example, reduced levels of the DNA dose in some areas of the Indian and Pacific Oceans correspond to 100% cloudy skies observed in these areas (see map of cloud fraction in Fig. 4). The cloudiness effect on the DNA dose is observed in the Mediterranean Sea -

where clear-sky conditions remained for more than a week, resulting in DNA dose values characteristic of equatorial regions.

It is interesting that the latitudinal distribution of both total ozone and the optical properties of ocean waters are not seen on the global DNA dose map. The effects of ozone amount and seawater optical properties are almost masked by cloudiness effects, indicating that latitudinal dependence of the UV irradiance and cloudiness are the major factors affecting the underwater DNA dose.

### 4.2 Z10 map

An important measure of the DNA dose is the depth at which DNA dose is reduced to 10% of its surface value (or Z10). This is the approximate depth over which biological damage due to UV effects take place. The 10% depth depends somewhat on the action spectrum used in calculations of UV dose rates. Since this dependence is rather weak, the 10% DNA dose depth can be used to characterize the biologically significant depth range.

A global map of the 10% DNA-dose depth is shown in Fig. 7a. Comparing this map with the chlorophyll and $K_d(490)$ maps, one can easily see that horizontal distribution of the 10% DNA dose depth is primarily determined by bio-optical properties of ocean waters. However, the angular structure of the light incident on the sea surface also affects the 10% DNA dose depth. This is because the dependence of the diffuse-attenuation coefficient on the angular structure of the in-water light field. The angular structure of the light incident on the sea surface is determined by the SZA and cloudiness. Therefore, a slight latitude dependence and cloudiness structure can be seen in the map of the 10% DNA dose depth.

A global map of Z10 is shown in Fig. 7b for unweighted UVB irradiance (280nm-320nm). The 10% UVB irradiance depth is normally greater than Z10 (the 10% DNA-dose depth). This is due to the fact that the integral over UVB irradiance is mainly determined by the longer wavelength part of UVB spectrum as opposed to the DNA dose that is mainly determined by shorter UVB wavelengths. The seawater is an effective filter of the shorter UV wavelengths.

Z10 is mainly determined by seawater IOPs rather then by the angular distribution of light incident on the sea surface. We carried out a sensitivity study intended to estimate the errors in Z10 due to uncertainties of the seawater IOPs.

The absorption coefficient of pure seawater has a strong affect on the UV penetration depth. To estimate the effect of its uncertainty on the UV penetration depth, data on the water absorption coefficient available in the spectral region of 340-380 nm [*Sogandares and Fry*, 1997] was extrapolated to 290-340 nm by using a least-squares technique applied to logarithms of the water absorption coefficient. Linear extrapolation resulted in lower values of the water absorption coefficient than logarithmic extrapolation. No absorption by salt, Chl a, or DOM was assumed. A comparison of the diffuse attenuation coefficient and penetration depths calculated for different water absorption coefficients is

shown in Figure 8, along with the diffuse attenuation coefficient measured in clear ocean waters [*Booth et al.*, 1992].

The Z10 UVB penetration depth calculated from the water absorption coefficient of *Sogandares and Fry* [1997] is about 20% greater than that calculated from coefficients of *Smith and Baker* [1981]. For example, the penetration depth at 320 nm is 29.9 m using the *Sogandares and Fry* [1997] data and 23.3 m for the Smith and Baker [1981] data. The 10% UVB depths are 24.2 m and 19.9 m respectively. It should be noted that the diffuse attenuation coefficients measured at 308, 320, and 340 nm are only slightly greater than those calculated using the *Sogandares and Fry* [1997] data. *Booth and Morrow* [1997] compared various measurements of the UV penetration in natural water and found no penetration depths at 320 nm greater than about 23m. This means that the 10% UVB irradiance depth generally should be less than 23 m. The only exception is data recently presented by *Aas and Hojerslev* [1999]. They reported of the 10% UVB irradiance depth as large as 35 m. The sensitivity study highlights the importance of accurate knowledge of the pure water absorption coefficient.

It is instructive to estimate how variations in the chlorophyll concentration and diffuse attenuation coefficient affect the UVB penetration depth. A contour plot of depths of UVB irradiance penetration to a level of 10% of its surface value is shown in Figure 9. In this case, the UVB penetration depth was calculated for the seawater absorption coefficient after *Smith and Baker* [1981]. No values of the UVB penetration depth for low $K_d(490)$ are available because the necessary condition $K_d > a + b_b$ is not valid [*Gordon*, 1989]. Calculations were conducted for two cases. In the first one, no CDOM absorption was assumed. The case represents upper limit values of the penetration depth. In the second case, it was assumed that the DOM absorption at 440 nm is 20% of the total absorption of pure seawater and pigments [*Morel*, 1988]. Figure 9 demonstrates the significant effect of the DOM absorption on the UVB penetration depth. For example, the UVB penetration depth for most probable chlorophyll concentration of 0.1 mg/m$^3$ and $K_d(490)$ = 0.03 m$^{-1}$ decreases from 17.4 m to 14.1 m. The DOM absorption reduces the maximum penetration depth from 19.9 m to 15.8 m.

## 5. Conclusions

A radiative transfer model for the atmosphere-ocean system has been developed for purpose of mapping underwater UV irradiance and biologically active UV dose rates in the ocean. The model is intended to combine total ozone and UV reflectivity measurements from TOMS, with ocean-color data available from CZCS and SeaWiFS. The ocean-color data includes monthly maps of chlorophyll concentration and the diffuse attenuation coefficient as well as daily maps of cloud fraction averaged on a grid of 1 by 1 degree.

The atmospheric part of the model generates spectral direct and diffuse irradiance on the sea surface that are inputs to the underwater part of the radiative transfer model. The in-water radiative transfer model is based on the QSSA (Quasi Single Scattering Approximation) that is simple, computationally fast, and yet enables the angular

distribution of the light field to be addressed. A model of seawater IOPs allows the extrapolation of the absorption and backscattering coefficients to the UV spectral region provided their values in the visible region are known. Values of the absorption and backscattering coefficients in the visible region are estimated from the SeaWiFS standard products by using the Case 1 water model.

The sensitivity study has shown that the main parameters controlling levels of the most harmful UV-B radiation underwater for clear sky conditions are the solar zenith angle, water bio-optical properties and total ozone. Attenuation of UV-B irradiance and DNA dose rate with water depth is primarily controlled by the seawater absorption coefficient and its spectral dependence. An influence of the seawater backscatter on the attenuation of UV irradiance is considerably less. Changes in the angular distribution of the surface radiance due to aerosol load or clouds may result in the irradiance increase at a given depth for large solar zenith angles. The sensitivity of UV-B and DNA dose rate to ozone variations decreases with depth.

The main spatial features of the weekly maps of underwater DNA dose are determined by the SZA and cloudiness. The seawater IOPs and total ozone effects are less significant for the spatial distribution of the DNA dose. The spatial distribution of the 10% DNA dose depth is mainly determined by the spatial structures of chlorophyll. Cloudiness effects and latitude dependence of the 10% DNA dose are also observed due to the effect of the angular distribution of the light incident on the sea surface in the in-water UV irradiance attenuation

**References**

Aas, E. and N.K. Hojerslev, Penetration of UVB irradiance into the Nordic Seas and adjacent coastal waters, *IUGG 99 Abstracts*, vol. B, B.244-B.255, 1999.

Arrigo, K.R., The impact of ozone depletion on phytoplankton growth in the Southern Ocean: Large-scale spatial and temporal variability, *Mar. Ecol. Prog. Ser.*, *114*, 1-12, 1994.

Arrigo, K. and C. McClain, Cloud and ice detection at high Latitudes for Processing CZCS imagery, SeaWiFS Algorithms, Part I, *NASA Tech. Memo 104566*, vol. 28, 38pp, 1995.

Barnes, R. A., A. W. Holmes, W. L. Barnes, W. E. Esaias and C. R. McClain, SeaWiFS Prelaunch Radiometric Calibration and Spectral Characterization, *NASA Tech. Memo. 104566*, vol. 23, 55 pp., 1994.

Barnes, R. A., R. E. Eplee, Jr., F. S. Patt, and C. R. McClain, Changes in the radiometric sensitivity of SeaWiFS, *Appl. Opt.*, *38*, 4649-4664, 1999.

Booth C.R., J.H.Morrow, and D.N.Neuschuler, A new profiling spectroradiometer optimized for use in the ultraviolet, *Ocean Optics XI, Proc. SPIE*, vol.1750, 354-365, 1992.

Booth C.R. and J.H. Morrow, Invited review: The penetration of UV into natural waters, *Photochem. Photobiol.*, 65, 254-257, 1997.

Bricaud A., M. Babin, A. Morel, and H. Claustre, "Variability in the chlorophyll-specific absorption coefficients of natural phytoplankton: analysis and parameterization," *J. Geophys. Res., 100*, 13,321-13,332, 1995.

Carder, K.L., S.K. Hawes, K.A. Baker, R.C. Smith, R.G. Steward, and B.G. Mitchell, Reflectance model for quantifying chlorophyll a in the presence of productivity degradation products, *J. Geophys. Res., 96*, 20,559-20,611, 1991.

Garver S. A. and D.A. Siegel, "Inherent optical property inversion of ocean color spectra and its biogeochemical interpretation: 1. Time series from the Sargasso Sea, " *J. Geophys. Res., 102*, 18,607-18,625, 1997.

Gordon H.R., Simple calculation of the diffusive reflectance of the ocean, *Appl. Opt., 12*, 2803-2804, 1973.

Gordon H.R. and A. Morel, Remote assessment of ocean color for interpretation of satellite visible imagery: a review, Springer-Verlag, New York, 114pp, 1983.

Gordon, H. R. and D. K. Clark, Clear water radiances for atmospheric correction of Coastal Zone Color Scanner imagery, *Appl. Opt., 20*, 4175-4180, 1981.

Gordon, H. R. and M. Wang, Retrieval of water-leaving radiance and aerosol optical thickness over the oceans with SeaWiFS: a preliminary algorithm, *Appl. Opt., 33*, 443-452, 1994.

Gordon H.R. Can the Lambert-Beer law be applied to the diffuse attenuation coefficient of ocean water? *Limnol. Oceanogr., 34*, 1389-1409,1989.

Greysukh, V.M., and I.M.Levin, The irradiance attenuation in the ocean and the diffused reflection coefficient, *Izvestiya USSR Academy of Science, Atmos. Oceanic Physics, 26*, 92-98, 1990.

Herman J.R.,P.K.Bhartia, Z. Ahmad, D.Larko, UV-B radiation increases (1979-1992) from decreases in total ozone, *Geophys. Res. Lett., 23*, 2,117 – 2,120, 1996

Herman et al., Global distribution of UV-Absorbing aerosols from Nimbus-7/TOMS data, *J. Geophys. Res., 102*, 16,911-16,922, 1997

Herman J.R., N.Krotkov, E.Celarier, D.Larko, and G.Labow, The distribution of UV radiation at the Earth's surface from TOMS measured UV-backscattered radiances, *J. Geophys. Res., 104*, 12,059-12,076, 1999

Hoge, F.E. and P.E. Lyon, Satellite retrieval of inherent optical propeties by linear matrix inversion of oceanic radiance models: an analysis of model and radiance measurement errors, *J. Geophys. Res., 101*, 16,631-16,648, 1996.

Hojerslev N.K. Yellow substance in the sea. In The Role Of Solar Ultraviolet Radiation In Marine Ecosystems, Ed. by J. Calkins, Plenum Press, 263-281, 1982.

Hojerslev N.K. Optical properties of sea water. *In: Landolt-Bornstein Numerical Data and Functional Relationships in Science and Technology*, Ed. by J. Sundermann, Springer Verlag, New Series, 3a, 1986.

Hojerslev N.K. and E. Aas A relationship for the penetration of ultraviolet B radiation into the Norwegian Sea. *J. Geoph. Res.*, **96**, 17,003-17,005, 1991.

Holm-Hansen, O., E. W. Helbling, D. Lubin, Ultraviolet radiation in Antarctica: Inhibition of primary production, *Photochem. Photobiol.*, **58**, 567-570, 1993.

Hooker, S. B., and C. R. McClain, A comprehensive plan for the calibration and validation of SeaWiFS data, *Prog. Oceanogr.*, in press, 1999.

Hooker, S.B., W.E. Esaias, G.C. Feldman, W.W. Gregg, and C.R. McClain, An overview of SeaWiFS and ocean color. *SeaWiFS Technical Report Series*, vol. 1, 24, 1992.

Johnson, B. C., E. E. Early, R. E. Eplee, Jr., R. A. Barnes, and R. T. Caffrey, The 1997 Prelaunch Radiometric Calibration of SeaWiFS, *NASA Tech. Memo. 1999-206892*, vol. 4, S. B. Hooker and E. R. Firestone (eds.), 51 pp., 1999.

Jin Z., and K.Stamnes, Radiative transfer in nonuniformly refracting layered media: atmosphere-ocean system, *Appl. Opt., 33*, 431-442, 1994

Kopelevich, O.V., S.V.Lutsarev, and V.V.Rodionov, Light spectral absorption by yellow substance of ocean water, *Oceanology, 29*, 409-414, 1989.

Kopelevich, O.V.and Yu.A. Filippov, Comparison between different spectral models of the diffuse attenuation and absorption coefficient of sea water, *Ocean Optics XII, Proc. SPIE*, edited by J. S. Jaffe, vol. 2258, 210-221, 1994.

Kopelevich O.V., and S. Ershova, Model of seawater optical characteristics in the UV spectral region. *Ocean Optics XIII, Proc. SPIE*, edited by S. G. Ackleson and R. Frouin, vol. 2963, 167-172, 1997.

Krotkov N.A. and A.P.Vasilkov, Theoretical model for prediction of ultraviolet radiation in the atmosphere-ocean system, *IRS'92: Current Problems in Atmospheric Radiation, Proc. IRS 1992*, A.DEEPAK Publ., 555-558, 1993

Krotkov N.A. and A.P.Vasilkov, Ultraviolet radiation in the atmosphere-ocean system: a model study, *Atmospheric Radiation, Proc SPIE*, edited by K. H. Stamnes, vol. 2049, 244-255, 1993.

Krotkov, N.A., P.K.Bhartia, J.R.Herman, V.Fioletov, J.Kerr, Satellite estimation of spectral surface UV irradiance in the presence of tropospheric aerosols 1. Cloud-free case, *J. Geophys. Res.*, ***103***, 8,779-8,793, 1998.

McClain, C.R., W.E.Esaias, W.Barnes, et al., SeaWiFS calibration and validation plan. *NASA Technical Memorandum 104566*, vol.3, 1992.

McClain, C. R., M. L. Cleave, G. C. Feldman, W. W. Gregg, S. B. Hooker, and N. Kuring, Science quality SeaWiFS data for global biosphere research, *Sea Technology, 39(9),* 10-16, 1998.

McKinlay, A.F. and B.L. Diffey A reference action spectrum for ultraviolet induced erythema in human skin. *Human Exposure to Ultraviolet Radiation: Risks and Regulations*, edited by W.R. Passchierand B.M. Bosnajakovich, 83-87, Elseiver, 1987.

Mueller, J. L. and C. C. Trees, Revised SeaWiFS prelaunch algorithm for the diffuse attenuation coefficient $K_d(490)$, *Case Studies for SeaWiFS Calibration and Validation, Part 4, NASA Tech. Memo. 104566*, vol. 41, edited by S. B. Hooker and E. R. Firestone, 18-21, 1997.

Mitchell, B.G., Action spectra of ultraviolet photoinhibition of Antarctic phytoplankton and a model of spectral diffuse attenuation coefficient," *Response of Marine Phytoplankton to Natural Variation in UV-B Flux, Proc. of Workshop,* edited by B.G.Mitchell, I.Sobolev, and O.Holm-Hansen, , Scripps Inst. of Oceanog., La Jolla, 1990.

Mobley, C.D., B.Gentili, H.R. Gordon, Z. Jin, G.W.Kattawar, A.Morel, P.Reinersman, K.Stamnes, and R.H.Stavn, Comparison of numerical models for computing underwater light fields, *Appl. Opt.*, *32*, 7,484-7,504, 1993.

Morel A., Optical modeling of the upper ocean in relation to its biogeneous matter content (Case I waters), *J. Geophys. Res.*, 93, 10,749-10,768, 1988.

Neale, P. J., R. F. Davis, J. J. Cullen, Interactive effects of ozone depletion and vertical mixing on photosynthesis of Antarctic phytoplankton, *Nature, 392*, 585-589, 1998.

Neale, P. J., J. J. Cullen, R. F. Davis, Inhibition of marine photosynthesis by ultraviolet radiation: Variable sensitivity of phytoplankton in the Weddell-Scotia Confluence during the austral spring, *Limnol. Oceanogr. 43*, 433-448, 1998.

O'Reilly, J. E., S. Maritorena, B. G. Mitchell, D. A. Siegel, K. L. Carder, S. A. Garver, M. Kahru, and C. McClain, Ocean color chlorophyll algorithms for SeaWiFS, *J. Geophys. Res., 103*, 24,937-24,953, 1998.

Pope R.M. and E.S. Fry, Absorption spectrum (380-700 nm) of pure water. II. Integrating cavity measurements, *Appl. Opt., 36*, 8710-8723, 1997.

Quaite, F.E., B.M.Sutherland and J.C.Sutherland, Action spectrum for DNA damage in alfalfa lowers predicted impact of ozone depletion, *Nature (Letters to Nature), 358*, 576-578, 1992.

Regan J.D., W.L.Carrier, H.Gucinski, B.L.Olla, H.Yoshida, R.K.Fujumura, and R.I.Wickland, DNA as a solar dosimeter in the ocean, *Photochem. Photobiol., 56*, 35-42, 1992.

Smith,R.C. and K.S.Baker, Penetration of UV-B and biologically effective dose-rates in natural waters, *Photochem. Photobiol., 29,* 311-323, 1979.

Smith R.C., and K.C.Baker, Optical properties of the clearest natural waters, *Appl. Opt., 20*, 177-186, 1981.

Smith, R.C., B.B.Prezelin, K.S.Baker, R.R.Biligare, N.P.Boucher, T.Coley, D.Karentz, S.MacIntyre, H.A.Matlic, D.Menzies, M.Ondrusek, Z.Wan, K.J.Waters, Ozone depletion: ultraviolet radiation and phytoplankton biology in Antarctic waters, *Science, 255*, 952-959, 1992.

Sogandares F.M. and E.S. Fry, "Absorption spectrum (340-700 nm) of pure water. I. Photothermal measurements," *Appl. Opt.*, 36, 8,710-8,723, 1997.

Stamnes, K.S., S.C. Tsay, W. Wiscombe, and K.Jayaweera, Numerically stable algorithm for discrete-ordinate-method radiative transfer in multiple scattering and emitting layered media, *Appl. Opt., 27*, 2502 - 2509, 1988.

Torres, O., P.K.Bhartia, J.R. Herman, Z.Ahmad, and J.Gleason, Derivation of aerosol properties from satellite measurements of backscattered ultraviolet radiation: Theoretical basis, *J. Geopgys. Res.,* **103**, 17099-17110, 1998

Vasilkov, A.P., A retrieval of coastal water constituent concentrations by least-squares inversion of a radiance model, *Proc. 4th Conference on Remote Sensing for Marine and Coastal Environments*, Orlando, 17-19 March 1997, Vol. 2, pp. 107-116, 1997.

Vasilkov A.P. and Krotkov N.A. Modeling the effect of seawater optical properties on the ultruviolet radiant fluxes in the ocean. *Izvestiya, Atmos. Ocean. Phys.*, , *33*, 349-357, 1997.

Vasilkov A.P., O.V. Kopelevich, N.A. Krotkov, S.V. Sheberstov, V.I. Burenkov, and S.V. Ershova, A model for calculations of ultraviolet radiative transfer in waters of the Arctic Seas. *Oceanology*, *39*, 192-201, 1999.

Vernet M., Brody E.A., Holm-Hansen O., Mitchell B.G. The response of antarctic phytoplankton to ultraviolet radiation: absorption, photosynthesis, and taxonomic composion. *Ultraviolet Radiation in Antarctica: Measurements and Biological Effects.* Antarctic Research Series. v.62. p.143-158, 1994.

Vodacek, A., and N.V. Blough, Seasonal variation of CDOM in the Middle Atlantic Bight: terrestrial inputs and photooxidation, *Ocean Optics XIII, Proc. SPIE*, edited by S. G. Ackleson and R. Frouin, vol. 2963, 132-137, 1997.

WMO98, Herman,J.R., R. L.McKenzie, S.B.Diaz, J.B.Kerr, S.Madronich, and G.Seckmeyer, Ultraviolet radiation at the Earth's surface, Chapter 9 In: Scientific Assessment of Ozone Depletion: 1998, *World Meteorological Organization, Global Ozone Research and Monitoring Project - Report N0.44*, Geneva, Switzerland, 1999.

Worrest, R.C. and D.P. Hader, Effect of stratospheric ozone depletion on marine organisms, *Environ. Conser.,16*, 261-263, 1989.

Zepp, R.G., and M.O.Andreae, Factors affecting the photochemical production of carbonyl sulfide in seawater, *Geophys. Res. Let.*, *21*, 2,813-2,816, 1994

## Figure Captions

Fig. 1. Data flow chart showing how TOMS and SeaWiFS products are assimilated by the suggested model.

Fig. 2. SeaWiFS-derived monthly chlorophyll *a* map for July 1998.

Fig. 3. SeaWiFS-derived monthly $K_d(490)$ map for July 1998.

Fig. 4. Map of the SeaWiFS-derived cloud fraction averaged over 5 days.

Fig. 5. TOMS-derived map of 5 day averaged surface UV irradiance from 290 to 400 nm weighted by the erythemal action spectra [*McKinlay and Diffey*, 1987]. The energy is expressed in kilojoules per square meter.

Fig. 6. Weekly averaged DNA dose map for July 1998. The DNA dose is expressed in a number of pyrimidine dimers produced per thousand bases of the DNA molecule during daytime.

Fig.7a. Map of the weekly averaged 10% DNA dose depth for July 1998.

Fig.7b. Map of the weekly averaged 10% UVB flux depth for July 1998.

Fig. 8. The diffuse attenuation coefficient and depth of penetration to level of 10% of the surface irradiance. Solid lines represent results calculated for the water absorption coefficient after *Smith and Baker* [1981]. Dashed lines represent results calculated for the extrapolated water absorption coefficient *after Sogandares and Fry* [1997]. Asterisks denote values measured for clear ocean waters [*Booth et al.*, 1992].

Fig. 9. The depth of UVB penetration to level of 10% of the surface irradiance as a function of the input parameters: chlorophyll concentration and the diffuse attenuation coefficient at 490 nm. (a) No DOM assumed. (b) DOM assumed to be according with the Case 1 water model [*Morel*, 1988].

**Popular Abstract**

# GLOBAL MAPPING OF UNDERWATER UV IRRADIANCES AND DNA-WEIGHTED EXPOSURES USING TOMS AND SEAWIFS DATA PRODUCTS

Alexander Vasilkov[1], Nickolay Krotkov[1], Jay Herman[2], Charles McClain[2], Kevin Arrigo[3], and Wayne Robinson[4]

**Abstract.** Global or local increases in penetration of UV radiation in the ocean can have harmful effects on the food chain. The global stratospheric ozone-layer depletion results in an increase in biologically harmful ultraviolet (UV) penetrating to ecologically significant depths in the ocean. Such an increase can be estimated anywhere in the Earth's oceans by combining satellite estimates of UV surface irradiance from the Total Ozone Mapping Spectrometer (TOMS) satellite instrument with the SeaWiFS satellite ocean-color measurements. We use a model of seawater optical properties with input from standard monthly SeaWiFS products: chlorophyll concentration and the diffuse attenuation coefficient at 490nm. Penetration of solar UV radiation to different depths in open ocean waters is calculated using an approximation to the full RT (radiative transfer) calculation with the results compared to more accurate models. We show that the the main environmental parameters controlling the absolute levels of the UVB (280-320nm) and DNA-weighted irradiance underwater are: solar-zenith angle, cloud transmittance, water optical properties, and total ozone. Weekly maps of underwater UV irradiance and DNA-weighted exposure are calculated using monthly-mean SeaWiFS chlorophyll and diffuse attenuation coefficient products, daily SeaWiFS cloud fraction data, and the TOMS-derived surface UV irradiance daily maps. The final products include global maps of weekly-average UVB irradiance and DNA-weighted daily exposures at ocean depths of 3m and 10m, and the depths where the UVB irradiance and DNA-weighted dose rate at local noon are equal to 10% of their surface values.

[1] Raytheon ITSS, Lanham, Maryland.
[2] NASA Goddard Space Flight Center, Greenbelt, Maryland.
[3] Department of Geophysics, Stanford University, Stanford, California
[4] SAIC General Sciences Co. and NASA/GSFC SeaWiFS Project, Greenbelt, Maryland.

# DATA FLOW CHART

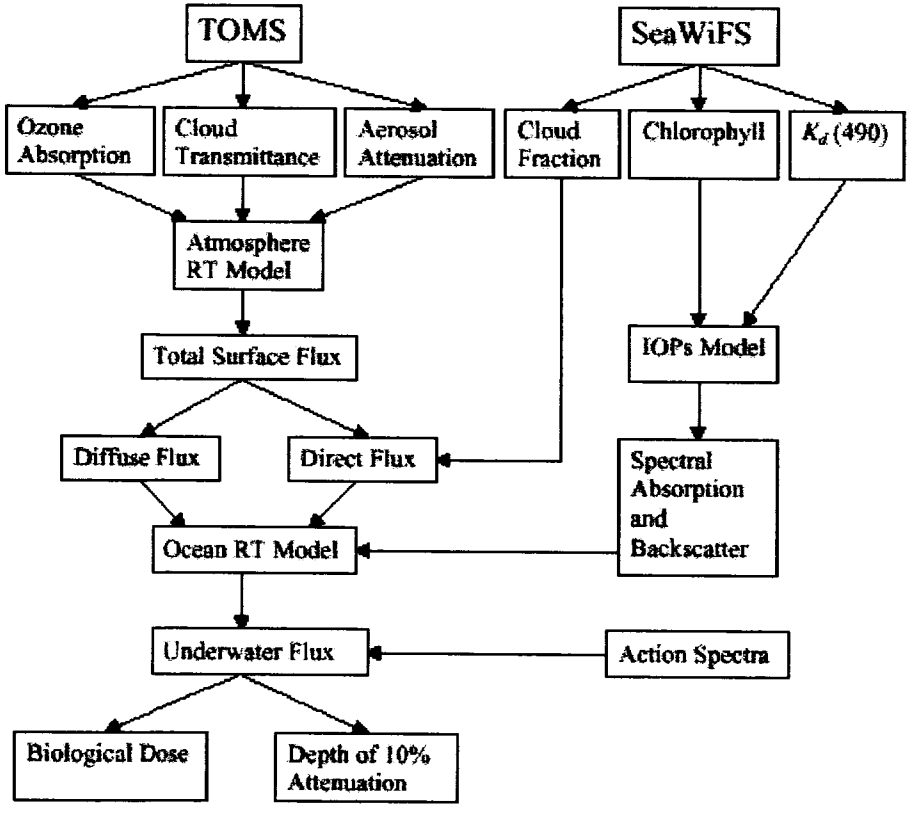


Figure 1

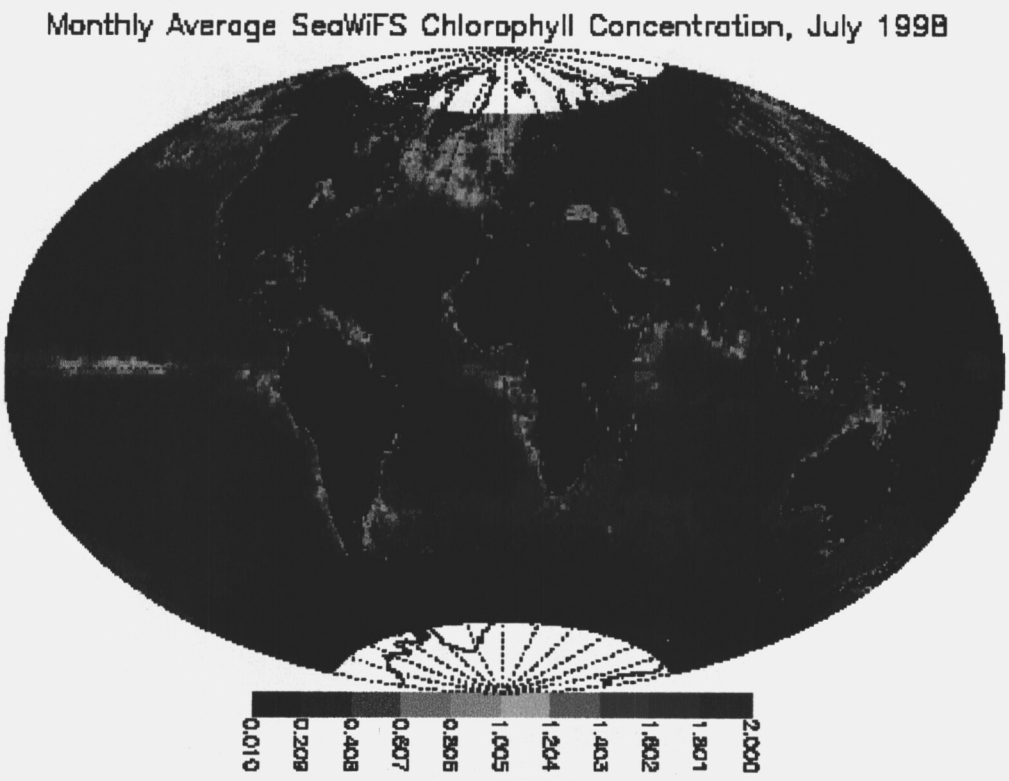
Monthly Average SeaWiFS Chlorophyll Concentration, July 1998
0.010
0.209
0.408
0.607
0.806
1.005
1.204
1.403
1.602
1.801
2.000

Figure 2

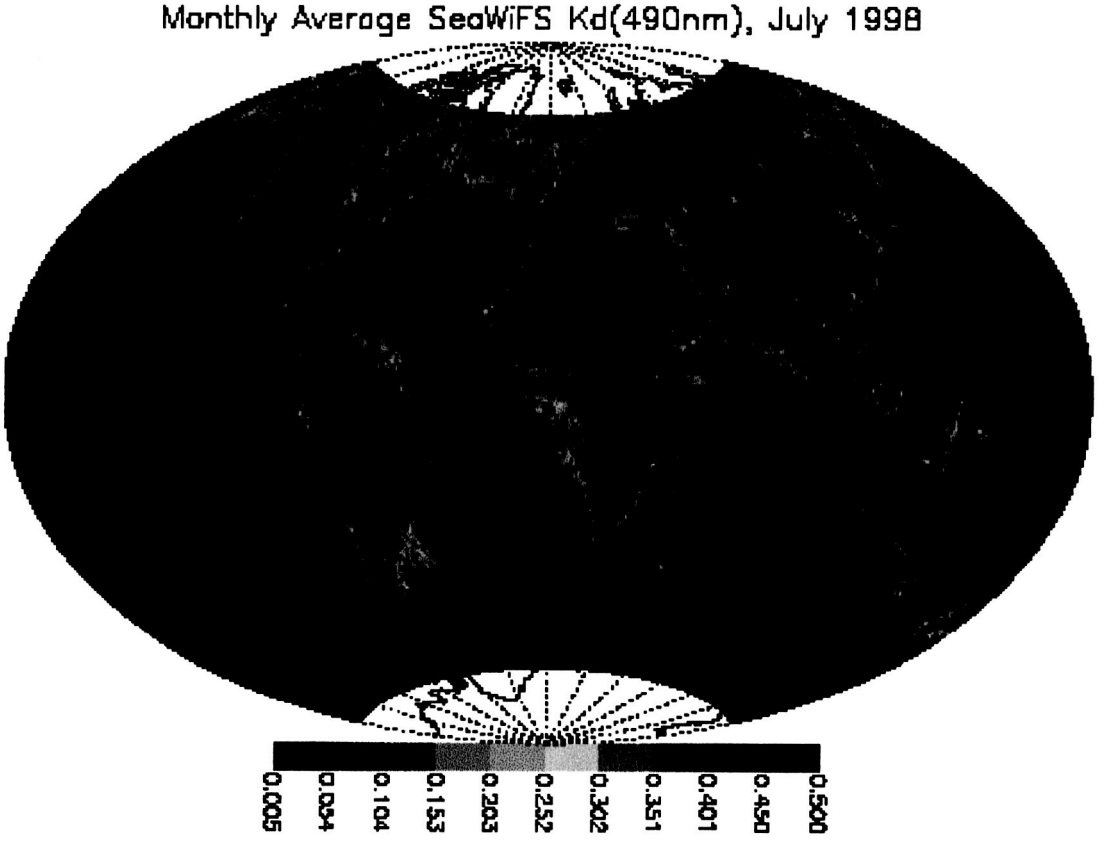
Monthly Average SeaWiFS Kd(490nm), July 1998
0.005
0.054
0.104
0.153
0.203
0.252
0.302
0.351
0.401
0.450
0.500

Figure 3

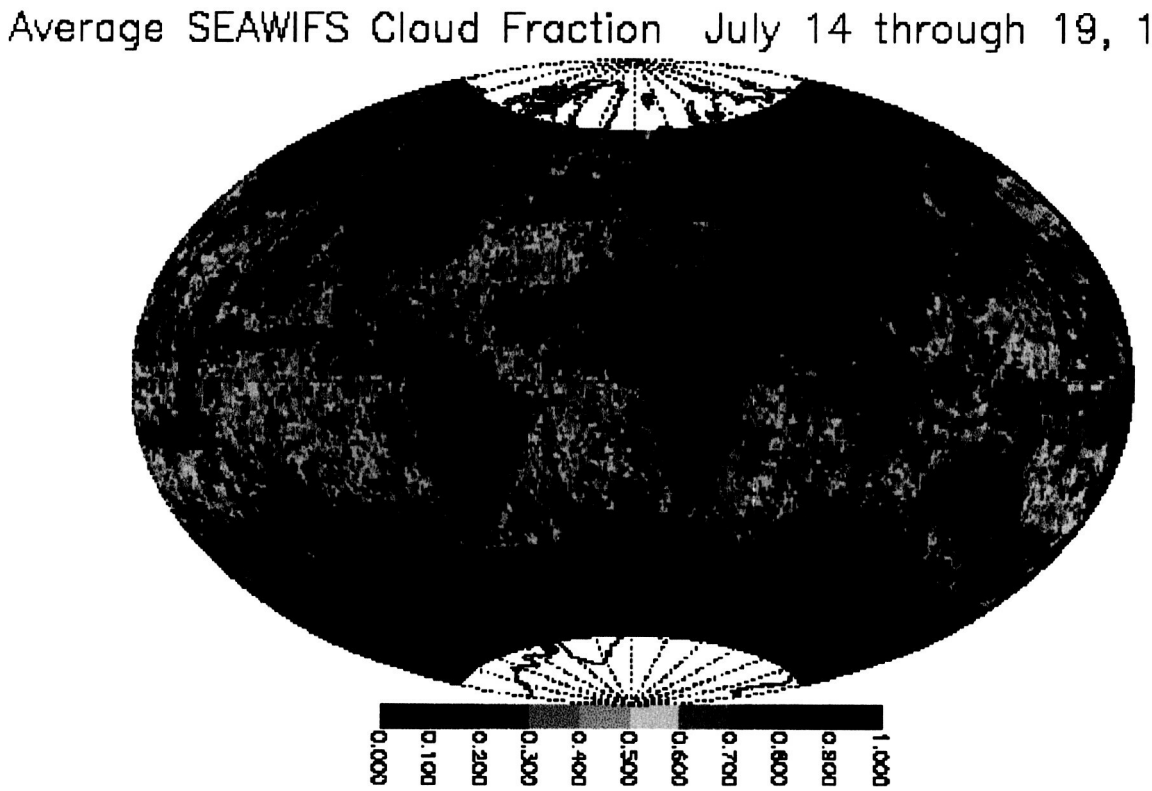
Average SEAWIFS Cloud Fraction July 14 through 19, 1998
0.000
0.100
0.200
0.300
0.400
0.500
0.600
0.700
0.800
0.900
1.000

**Figure 4**

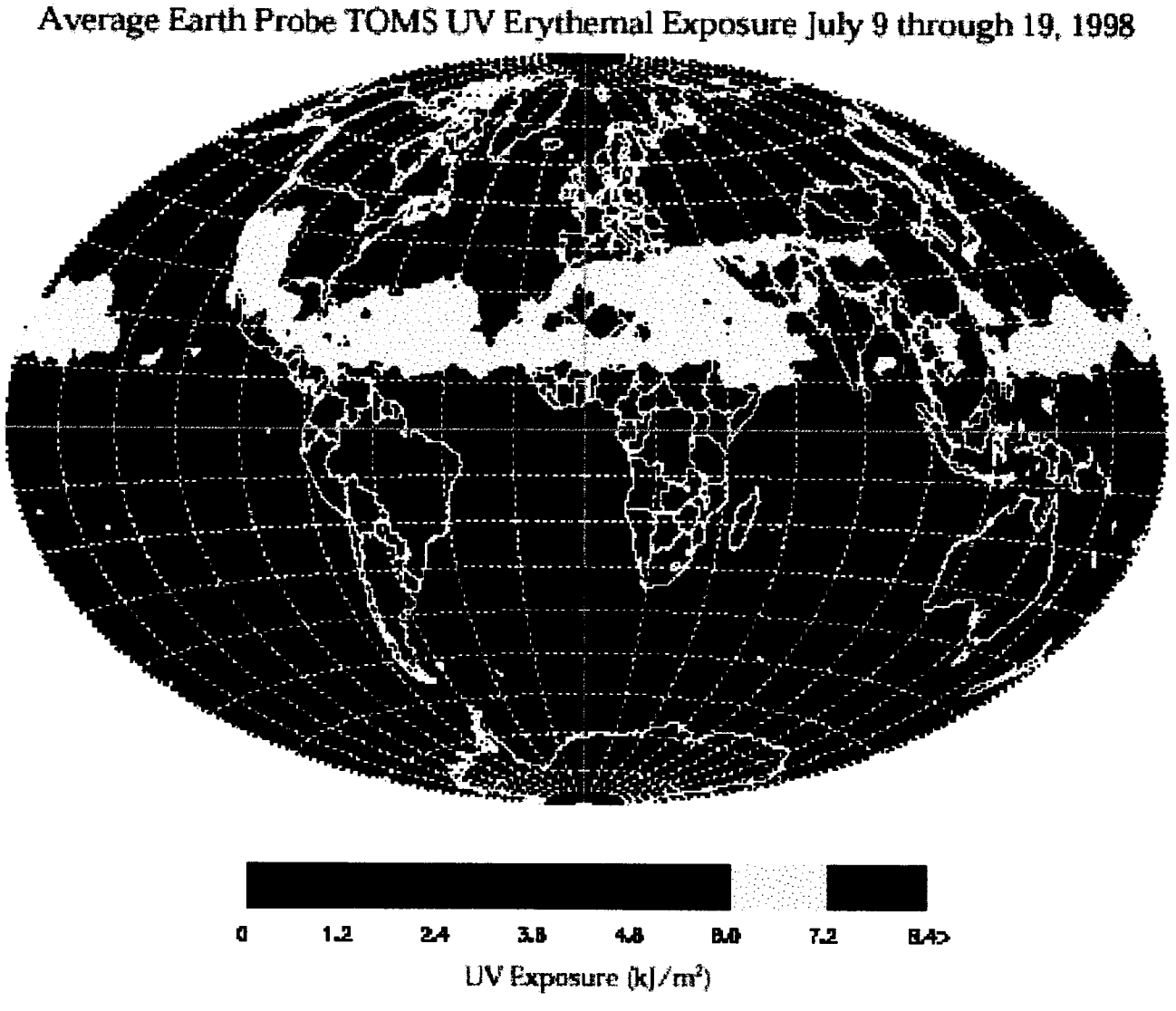
Average Earth Probe TOMS UV Erythemal Exposure July 9 through 19, 1998
0
1.2
2.4
3.6
4.8
6.0
7.2
8.4>
UV Exposure (kJ/m²)

Figure 5

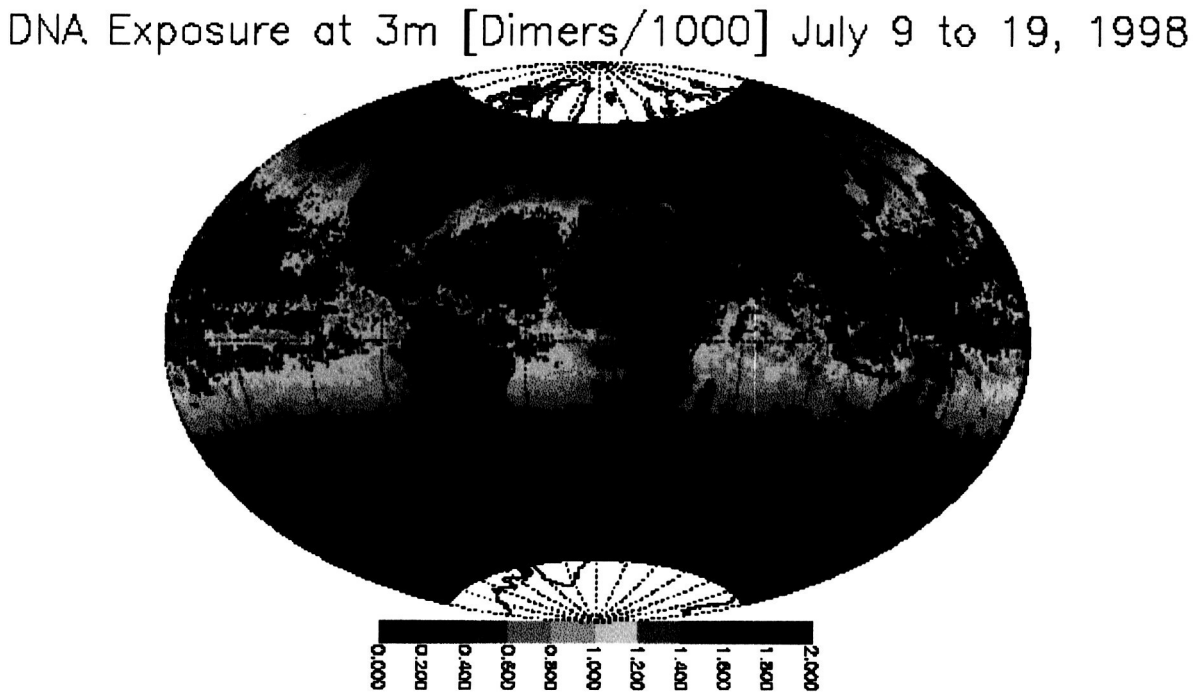
DNA Exposure at 3m [Dimers/1000] July 9 to 19, 1998
0.000
0.200
0.400
0.600
0.800
1.000
1.200
1.400
1.600
1.800
2.000

**Figure 6**

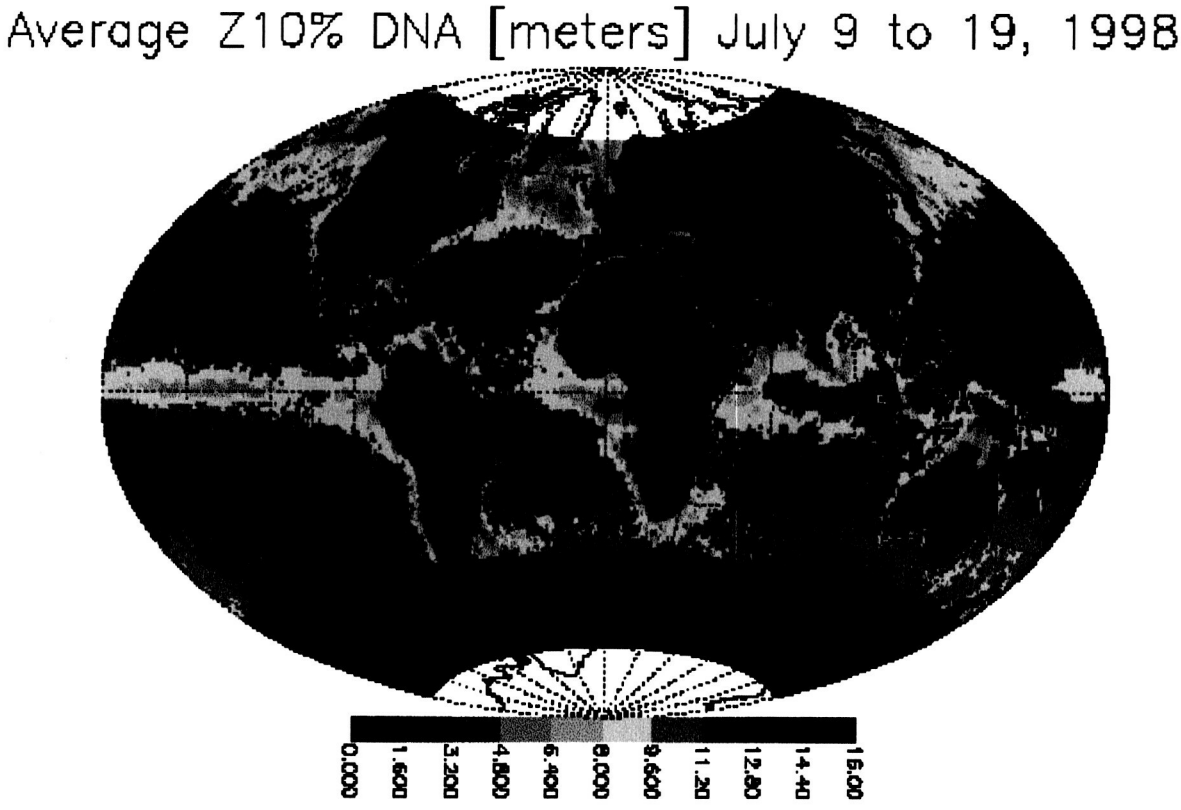
Average Z10% DNA [meters] July 9 to 19, 1998
0.000
1.600
3.200
4.800
6.400
8.000
9.600
11.20
12.80
14.40
16.00

Figure 7a

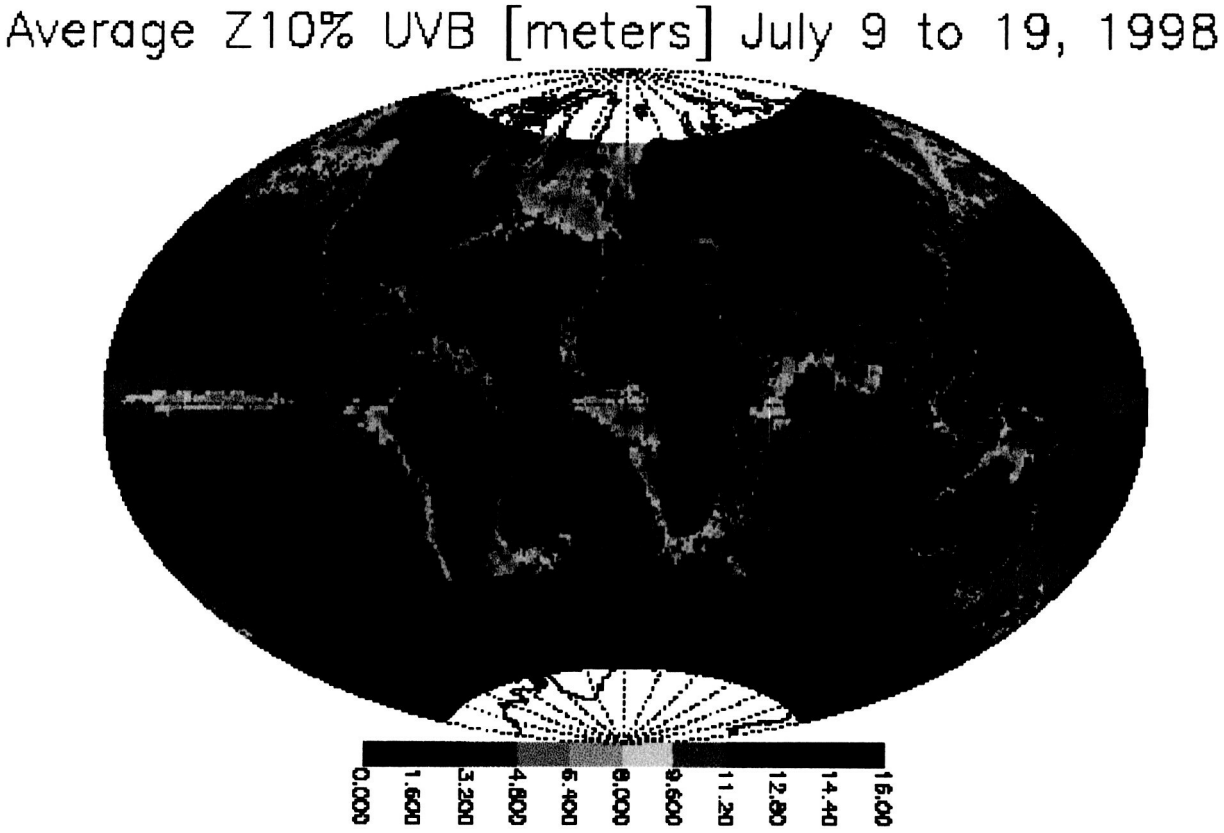
Average Z10% UVB [meters] July 9 to 19, 1998
0.000
1.600
3.200
4.800
6.400
8.000
9.600
11.20
12.80
14.40
16.00

Figure 7b

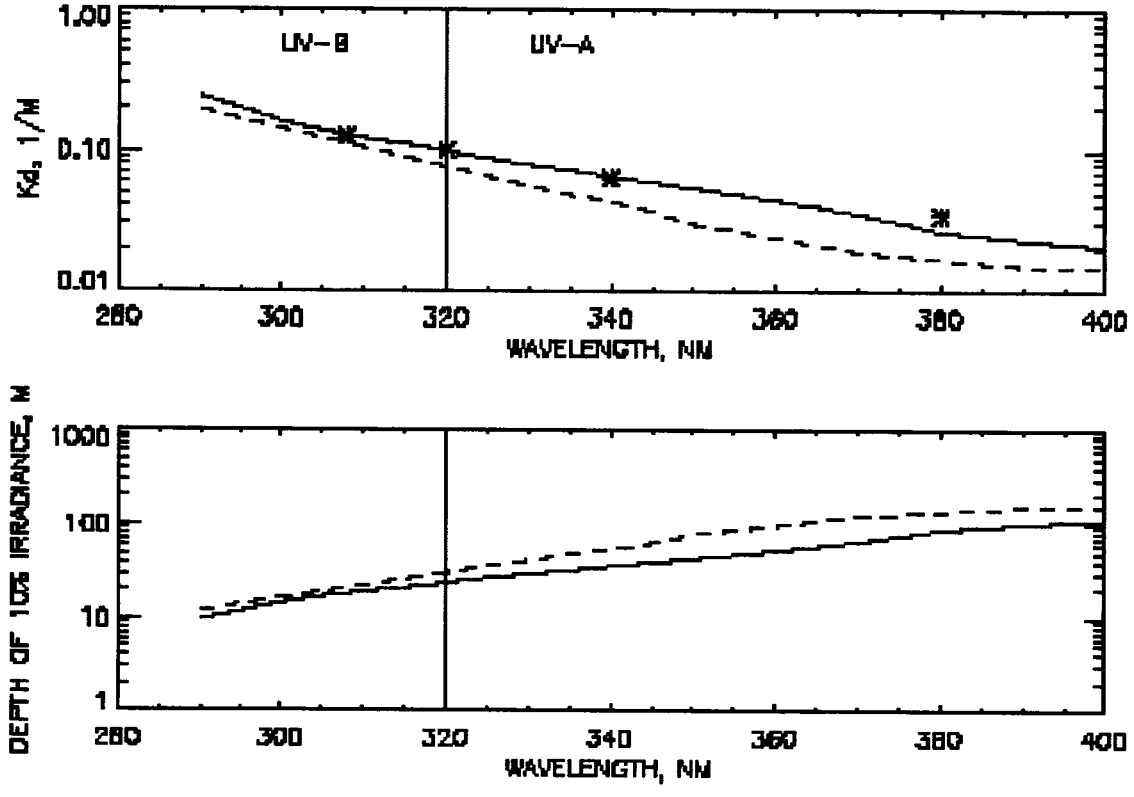
1.00
0.10
0.01
Kd, 1/M
UV-B
UV-A
280
300
320
340
360
380
400
WAVELENGTH, NM
1000
100
10
1
DEPTH OF 10% IRRADIANCE, M
280
300
320
340
360
380
400
WAVELENGTH, NM

Figure 8

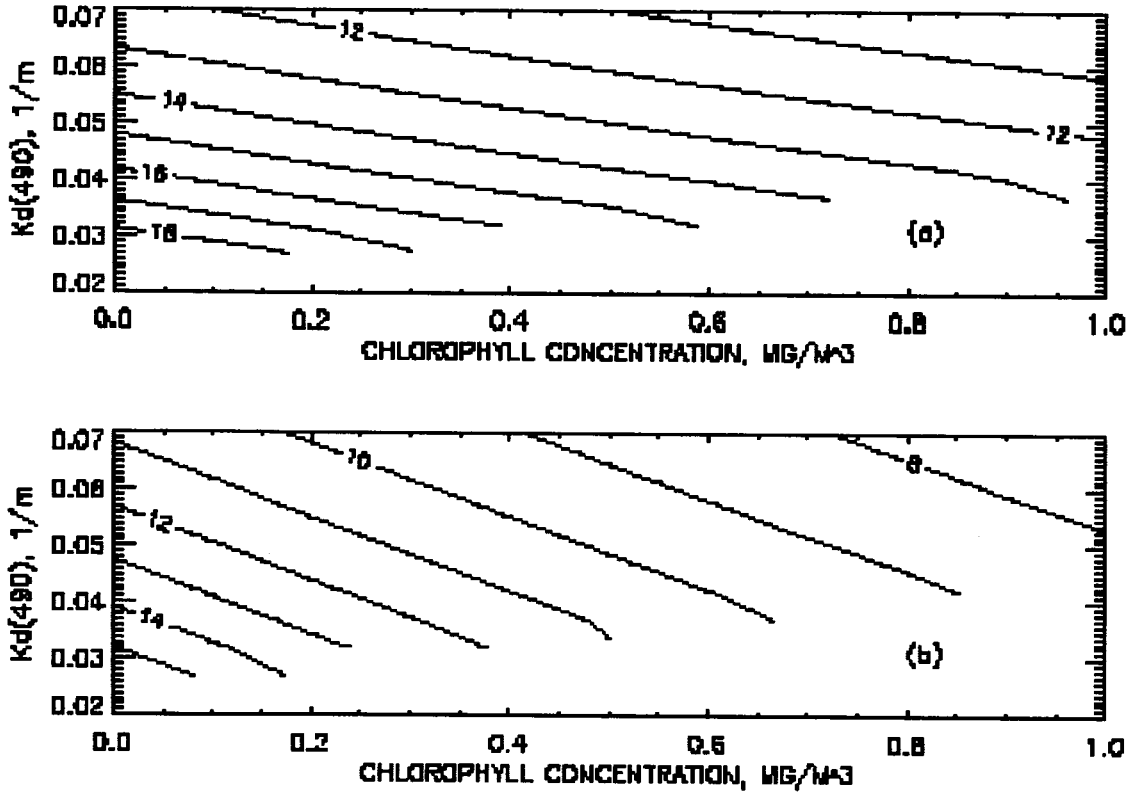
0.07
0.06
0.05
0.04
0.03
0.02
Kd(490), 1/m
12
14
16
18
12
(a)
0.0
0.2
0.4
0.6
0.8
1.0
CHLOROPHYLL CONCENTRATION, MG/M^3
0.07
0.06
0.05
0.04
0.03
0.02
Kd(490), 1/m
10
8
12
14
(b)
0.0
0.2
0.4
0.6
0.8
1.0
CHLOROPHYLL CONCENTRATION, MG/M^3

Figure 9